Articles published week of 28 FEBRUARY 2011
Volume 98 Number 9

APPLIED PHYSICS LETTERS

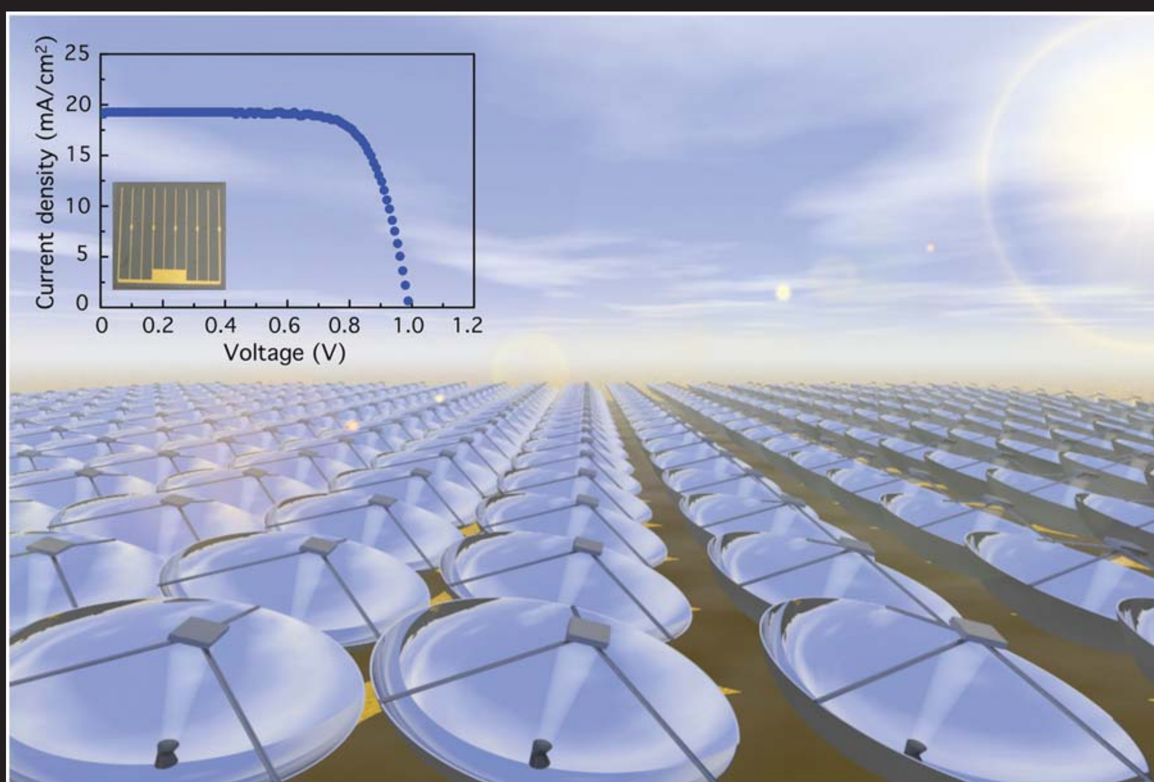

AIP

APPLIED PHYSICS LETTERS **98**, 093502 (2011)

Wide-band-gap InAlAs solar cell for an alternative multijunction approach

Marina S. Leite,[1,a)] Robyn L. Woo,[2] William D. Hong,[2] Daniel C. Law,[2] and Harry A. Atwater[1]
[1]*California Institute of Technology, 1200 E. California Blvd., Pasadena, California 91125, USA*
[2]*Boeing-Spectrolab Inc., 12500 Gladstone Avenue, Sylmar, California 91342, USA*

(Received 23 September 2010; accepted 5 December 2010; published online 28 February 2011)

We have fabricated an $In_{0.52}Al_{0.48}As$ solar cell lattice-matched to InP with efficiency higher than 14% and maximum external quantum efficiency equal to 81%. High quality, dislocation-free $In_xAl_{1-x}As$ alloyed layers were used to fabricate the single junction solar cell. Photoluminescence of $In_xAl_{1-x}As$ showed good material quality and lifetime of over 200 ps. A high band gap $In_{0.35}Al_{0.65}As$ window was used to increase light absorption within the *p-n* absorber layer and improve cell efficiency, despite strain. The InAlAs top cell reported here is a key building block for an InP-based three junction high efficiency solar cell consisting of InAlAs/InGaAsP/InGaAs lattice-matched to the substrate. © *2011 American Institute of Physics*. [doi:10.1063/1.3531756]

The need for high efficiency photovoltaics has recently attracted considerable interest in multijunction solar cells based on III-V semiconductors.[1] Such devices can achieve efficiencies over 40% under AM 1.5 global illumination[2] and can potentially be used both in terrestrial and spacial applications. Usually, multijunction solar cell designs are based on materials grown in Ge or GaAs[3] due to the well understood optical and electronic properties of the lattice-matched alloys. The most common configuration consists of a top InGaP cell, a middle GaAs cell, and a Ge bottom cell, with modeled efficiency up to 40% under 1 sun illumination.[4,5] However, the large bandgap difference between Ge and GaAs leads to poor current matching between these subcells in a multijunction solar cell design. Direct wafer bonding combined with layer transfer has been proposed to integrate subcells with distinct lattice spacing.[6] Also, inverted metamorphic growth allows for the fabrication of GaInP/GaAs/InGaAs triple junction cells with efficiencies higher than 30% under 1-sun illumination.[7] Additionally, by adding two independent metamorphic junctions, an efficiency over 40% was achieved.[8] In this approach, current matching is optimized for a lattice-mismatched $In_xGa_{1-x}As$ bottom junction. Therefore, a graded InGaP buffer layer is required prior to bottom cell growth, which can result in dislocations depending on the material growth conditions. Additionally, growth of a thick grade layer adds to the total growth time and cost in a commercial setting.

In order to enable excellent current matching between the middle and bottom subcells and also to work with lattice-matched epitaxial layers, we propose an alternative InP-based approach for a triple junction solar cell formed by a combination of InAlAs(1.47 eV)/InGaAsP(1.06 eV)/InGaAs(0.74 eV) alloys. Detailed balance calculations indicate that this multijunction solar cell can achieve over 46% efficiency at 100 suns illumination with subcells connected in series.[9] Here, we present an InAlAs solar cell lattice-matched to InP which is a promising option for a top junction in an InP-based multijunction configuration. We discuss in detail the material crystal quality and optical properties. Solar cells were fabricated with an efficiency of 14.2% at AM 1.5 1 sun illumination and maximum external quantum efficiency of 81.0%. This performance is attributed to the high bandgap top window which reduces surface recombination and increases light absorption within the *p-n* absorber layer despite an increase in strain. The overall performance of the cell supports the possibility of a high efficiency InAlAs/InGaAsP/InGaAs triple junction cell.

$In_xAl_{1-x}As$ alloys have been used as window layers in low bandgap InGaAs solar cells[10] and showed very good efficiencies. It was also suggested[11] that a wide-band-gap $In_xAl_{1-x}As$ window layer could boost the efficiency of InP solar cells by more than 20% due to the almost negligible window layer light absorption. Figure 1 shows a schematic and a photograph of the fabricated InAlAs solar cells. The single junction InAlAs solar cells were grown on 50 mm, *p*-type InP (001) on-axis substrates using Veeco E400 metal-organic vapor phase epitaxy reactor operated at low pressure. The main precursors used in the layers are trimethylindium, trimethylaluminum, and arsine. Growth temperatures typically ranged from 600 to 750 °C depending on the layers. The *p-n* absorber layer consists of an $In_{0.52}Al_{0.48}As$ *n*-doped layer 200 nm thick with a carrier concentration of 1.0

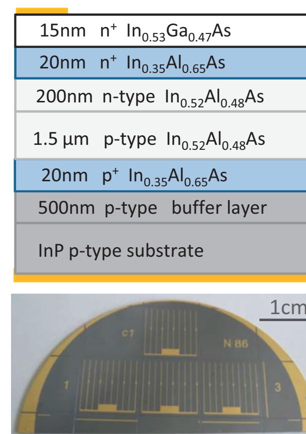

FIG. 1. (Color) Top: Schematic of InAlAs/InP solar cell showing layer thickness and composition. Blue: $In_{0.35}Al_{0.65}As$ window layers $\rightarrow E_g = 1.98$ eV. Light gray: $In_{0.52}Al_{0.47}As$ *p-n* absorber layer $\rightarrow E_g = 1.47$ eV. White: $In_{0.53}Ga_{0.47}As$ cap layer $\rightarrow E_g = 0.77$ eV. Yellow: metallic contacts. Bottom: Photograph of fabricated InAlAs solar cells with 1×1 cm^2 each.

a)Electronic mail: mleite@caltech.edu.

 © 2011 American Institute of Physics

Downloaded 15 Mar 2011 to 131.215.220.161. Redistribution subject to AIP license or copyright; see http://apl.aip.org/about/rights_and_permissions

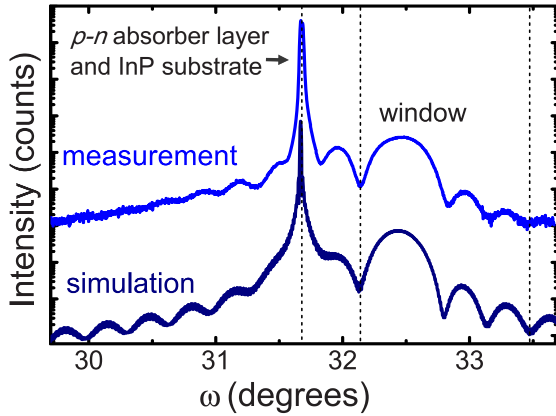

FIG. 2. (Color online) X-ray diffraction measurement and simulation of the cell structure showing a pseudomorphic window layer. Window broad peak and fringes correspond to a 20 nm unrelaxed $In_{0.35}Al_{0.65}As$ layer. Measurement settings: lambda=1.540 56 Å, (0 0 4) reflection, receiving slit: 1/2°.

$\times 10^{18}$ cm^{-3} and a 1.5 μm thick layer with the same composition, p-doped with 1.0×10^{17} cm^{-3}. The junction is sandwiched by a top $In_{0.35}Al_{0.65}As$ window layer 20 nm thick and a back surface field with the same thickness and composition. The top layer is highly doped to minimize surface recombination.

The $In_{0.35}Al_{0.65}As$ alloy used for the window layer has a lattice spacing of 5.8001 Å, being 1.17% tensile with respect to the InP substrate and the p-n absorber layer. Figure 2 shows an x-ray diffraction ω-2θ measurement at (0 0 4) reflection for the InAlAs solar cell. The p-n absorber layer peak is superposed to the substrate sharp peak, confirming that the $In_{0.52}Al_{0.48}As$ layer is lattice-matched to InP. The window layer diffraction condition (broad peak and fringes) demonstrates that this layer is coherently-strained with respect to InP and corresponds to a 20 nm thick $In_{0.35}Al_{0.65}As$ alloy, matching the nominal composition. As shown in Fig. 2 the measurement is in very good agreement with x-ray simulation for a similar unrelaxed structure. Therefore, although the $In_{0.35}Al_{0.65}As$ window is highly strained with respect to the InP substrate (+1.17%) it is below the critical thickness for the kinetic growth conditions used and is therefore dislocation-free. A pseudomorphic and defect-free wide-band-gap window is ideally suited to reduce surface recombination velocity. The dependence of $In_xAl_{1-x}As$ bandgap energy with material lattice spacing indicates that a small increase in strain can abruptly increase the window bandgap and, as a consequence, reduce parasitic window light absorption by this layer.

The $In_{0.52}Al_{0.48}As$ alloy optical properties were investigated by room temperature photoluminescence. Very little optical information is available for $In_xAl_{1-x}As$ alloys. Figure 3(a) shows the photoluminescence spectrum for a p-type $In_{0.52}Al_{0.48}As$/InP double heterostructure. The peak at 1.34 eV is due to the InP substrate; 1.47 eV corresponds to the $In_{0.52}Al_{0.48}As$ layer. The interface between InAlAs and InP results in a thin InAsP layer which gives rise to a lower energy luminescence band at 1.23 eV. This peak is known to be due to a mixed type I-II heterostructure recombination.[12] The well defined peaks demonstrate the optical quality of the grown $In_{0.52}Al_{0.48}As$. Time-resolved room temperature photoluminescence measurements for the same alloy showed an exponential decay with a lifetime of 206 ps, as in Fig. 3(b). In order to determine the minority carrier diffusion length of

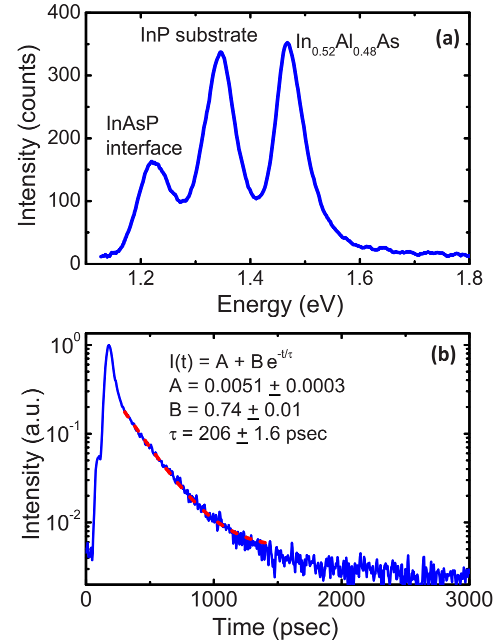

FIG. 3. (Color online) (a) Room temperature photoluminescence measurement of the $In_{0.52}Al_{0.48}As$ 300 nm layer as a function of wavelength showing material bandgap and alloy/InP interface peak. (b) Time-resolved photoluminescence measurement on the same alloy showing a lifetime of 206 ps. The dashed line corresponds to the exponential decay behavior.

$In_{0.52}Al_{0.48}As$ alloy, Hall measurements were taken in a 930 nm thick $In_{0.52}Al_{0.48}As$ n-doped layer. Hall mobility was measured to be 667 ± 8 cm^2/V s for $N_d=(2.68\pm 0.02)\times 10^{18}$ cm^{-3} carrier density. Therefore we estimate a lower bond on the minority carrier diffusion length in the $In_{0.52}Al_{0.48}As$ alloy grown of approximately 1 μm.

One dimensional device modeling was performed[13,14] in order to assess the performance of $In_xAl_{1-x}As$ wide-band-gap window layers. The results are shown in Table I for $In_{0.52}Al_{0.48}As$ solar cells lattice-matched to InP with a structure similar to the one presented in Fig. 1. The effect of a 20 nm thick $In_{0.35}Al_{0.65}As$ window layer was investigated, which can be synthesized dislocation-free, depending on specific growth conditions. According to the device modeling, the overall cell performance is strongly affected by the presence of the Al-rich top window layer [see Fig. 4(a) for light I-V experimental curves]. In the absence of a top window, the short circuit current (J_{sc}) is significantly reduced due to surface recombination in the n-type layer of the cell, and cell efficiency η decreases (10.7%). According to the device modeling, an $In_{0.35}Al_{0.65}As$ window can boost cell efficiency to 19.6%.[15]

In order to improve the top contact of the cell a thin InGaAs contact layer was used.[10] Although the low bandgap (0.74 eV) of this layer causes parasitic absorption to the solar cell, overall cell performance was significantly improved compared to a cell without the cap layer. Electrical measurements were performed using a solar simulator with active illumination area under AM 1.5 global solar spectrum with 1 sun total intensity (100 mW/cm^2). Figure 4(a) shows a light I-V curve for a representative cell with 1.0 cm^2. InAlAs solar cell photovoltaic characteristics are maximum power P_m =14.2 mW/cm^2 with V_{mp}=809.0 mV and J_{mp} =17.5 mA/cm^2. An open circuit voltage (V_{oc}) of 990 mV and a short circuit current density (J_{sc}) of 19.3 mA/cm^2

Downloaded 15 Mar 2011 to 131.215.220.161. Redistribution subject to AIP license or copyright; see http://apl.aip.org/about/rights_and_permissions

TABLE I. InAlAs solar cell figures of merit obtained by one device modeling[14] of the structure shown in Fig. 1 without and with a 20 nm thick InAlAs top window layer with different compositions and therefore band gap energies. The modeling takes multiple internal and external reflections into account and normal incidence of light. The last row shows the parameter measured for the InAlAs solar cell with $In_{0.35}Al_{0.65}As$ windows, $In_{0.53}Ga_{0.47}As$ cap layer, and an antireflection coating. In all cases EQE refers to the maximum value of the external quantum efficiency achieved at 765 nm.

	V_{oc} (mV)	J_{sc} (mA/cm^2)	FF (%)	η (%)	EQE (%)
Without top window	984	12.6	87	10.7	53.4
With 1.7 eV top window	1017	19.8	88	17.7	68.0
With 2.0 eV top window	1064	20.8	89	19.6	82.0
Experiment	990	19.3	74.4	14.2	81.0

were measured. The resulting cell efficiency is 14.2% with fill factor (FF) of 74.4%, promising for a wide-band-gap top junction cell. The fabricated InAlAs cells were found to be very stable under ambient conditions. An external quantum efficiency (EQE) of 81.0% was achieved for the same cell [see Fig. 4(b)]. The EQE drops rapidly for wavelength >828 nm as a consequence of $In_{0.52}Al_{0.48}As$ bandgap energy.

The overall cell efficiency is higher than for cells using lower bandgap window layers. An $In_{0.47}Al_{0.53}As$ window with $E_g=1.76$ eV and a lattice mismatch of +0.37% with respect to InP resulted in a relative efficiency that was 18% lower [see Fig. 4(a)]. The high bandgap of the $In_{0.35}Al_{0.65}As$ window layer allows for more light absorption in the *p-n* absorber layer. Additionally, the EQE improved by 5% in the blue region of the spectrum (not shown).

Summarizing, by controlling defects such as dislocations in $In_xAl_{1-x}As$ layers with different compositions we fabricated a wide-band-gap InAlAs solar cell. The InAlAs *p-n* absorber layer was lattice-matched to the InP substrate and a top $In_{0.35}Al_{0.65}As$ window layer was used to prevent surface recombination and provide more light absorption into the absorber layer. High quality material was achieved from both structural and optical properties' standpoints. The InAlAs fabricated solar cells showed an efficiency of 14.2% and an EQE of up to 81.0%. The demonstration of an InAlAs wide-band-gap solar cell presented here opens up the possibility for an innovative multijunction solar cell design based on InP lattice-matched alloys.

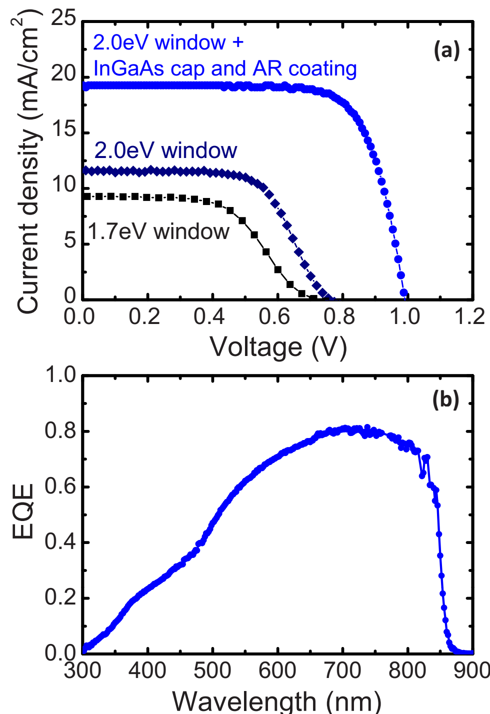

FIG. 4. (Color online) (a) Light I-V curve under AM 1.5 global illumination for the fabricated InAlAs solar cells using a 1.7 eV window layer (squares), a 2.0 eV window layer (diamonds), and a 2.0 eV window plus an InGaAs cap layer and antireflection (AR) coating (circles). Best cell characteristics are shown in Table I. (b) External quantum efficiency (EQE) of the InAlAs cell with cap layer and AR coating as a function of light wavelength.

The authors acknowledge D. M. Callahan, J. S. Fakonas, G. M. Kimball, J. N. Munday, and D. M. O'Carroll and financial support from the Department of Energy—Solar Energy Technologies Program under Grant No. DE-FG36-08GO18071.

[1]R. R. King, Nat. Photonics **2**, 284 (2008).
[2]M. J. Griggs, D. C. Law, R. R. King, A. C. Ackerman, J. M. Zahler, and H. A. Atwater, *Proceedings of the 4th World Conference on Photovoltaic Energy Conversion* (IEEE, New York, 2006), p. 857.
[3]J. Olson, T. Gessert, and M. Al-Jassim, *Proceedings of the 18th IEEE Photovoltaic Specialists Conference* (IEEE, New York, 1985), p. 552.
[4]F. Dimroth, U. Schubert, and A. W. Bett, IEEE Electron Device Lett. **21**, 209 (2000).
[5]*Handbook of Photovoltaic Science and Engineering*, edited by A. Luque and S. Hegedus (Wiley, West Sussex, England, 2003).
[6]D. C. Law, R. R. King, H. Yoon, M. J. Archer, A. Boca, C. M. Fetzer, S. Mesropian, T. Isshiki, M. Haddad, K. M. Edmondson, D. Bhusari, J. Yen, R. A. Sherif, H. A. Atwater, and N. H. Karam, Sol. Energy Mater. Sol. Cells **94**, 1314 (2010).
[7]J. F. Geisz, S. Kurtz, M. W. Wanlass, J. S. Ward, A. Duda, D. J. Friedman, J. M. Olson, W. E. McMahon, T. E. Moriarty, and J. T. Kiehl, Appl. Phys. Lett. **91**, 023502 (2007).
[8]J. F. Geisz, D. J. Friedman, J. S. Ward, A. Duda, W. J. Olavarria, T. E. Moriarty, J. T. Kiehl, M. J. Romero, A. G. Norman, and K. M. Jones, Appl. Phys. Lett. **93**, 123505 (2008).
[9]M. J. Archer (private communication).
[10]Y. Takeda, M. Wakai, T. Ikeoku, and A. Sasaki, Sol. Energy Mater. Sol. Cells **26**, 99 (1992).
[11]R. K. Jain, G. A. Landis, D. M. Wilt, and D. J. Flood, Appl. Phys. Lett. **64**, 1708 (1994).
[12]D. Vignaud, X. Wallart, F. Mollot, and B. Sermage, J. Appl. Phys. **84**, 2138 (1998).
[13]Modeling was performed using automat for simulation of heterostructures (AFORS-HET) free software.
[14]R. Stangl, M. Kriegel, and M. Schmidt, *Proceedings of the 4th World Conference on Photovoltaic Energy Conversion* (IEEE, New York, 2006), p. 1350.
[15]The purpose of the modeling presented here is to determine quantitatively how a top window can affect the overall cell performance; therefore no antireflection coating was included on the simulations.

Downloaded 15 Mar 2011 to 131.215.220.161. Redistribution subject to AIP license or copyright; see http://apl.aip.org/about/rights_and_permissions